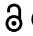







ORIGINAL RESEARCH

 OPEN ACCESS 

Converging focal radiation and immunotherapy in a preclinical model of triple negative breast cancer: contribution of VISTA blockade

Karsten A. Pilonis ^a, Michal Hensler ^b, Camille Daviaud^a, Jeffrey Kravak^a, Jitka Fucikova^{b,c}, Lorenzo Galluzzi^{a,d,e}, Sandra Demaria ^{a,d,f}, and Silvia C. Formenti ^{a,d}

^aDepartment of Radiation Oncology, Weill Cornell Medical College, New York, NY, USA; ^bSotio, Prague, Czech Republic; ^cDepartment of Immunology, Charles University, 2nd Faculty of Medicine and University Hospital Motol, Prague, Czech Republic; ^dSandra and Edward Meyer Cancer Center, New York, NY, USA; ^eCaryl and Isreal Englander Institute for Precision Medicine, Weill Cornell Medical College, New York, NY, USA; ^fDepartment of Pathology and Laboratory Medicine, Weill Cornell Medical College, New York, NY, USA

ABSTRACT

Antibodies targeting the co-inhibitory receptor programmed cell death 1 (PDCD1, best known as PD-1) or its main ligand CD274 (best known as PD-L1) have shown some activity in patients with metastatic triple-negative breast cancer (TNBC), especially in a recent Phase III clinical trial combining PD-L1 blockade with taxane-based chemotherapy. Despite these encouraging findings, however, most patients with TNBC fail to derive significant benefits from PD-L1 blockade, calling for the identification of novel therapeutic approaches. Here, we used the 4T1 murine mammary cancer model of metastatic and immune-resistant TNBC to test whether focal radiation therapy (RT), a powerful inducer of immunogenic cell death, in combination with various immunotherapeutic strategies can overcome resistance to immune checkpoint blockade. Our results suggest that focal RT enhances the therapeutic effects of PD-1 blockade against primary 4T1 tumors and their metastases. Similarly, the efficacy of an antibody specific for V-set immunoregulatory receptor (VSIR, another co-inhibitory receptor best known as VISTA) was enhanced by focal RT. Administration of cyclophosphamide plus RT and dual PD-1/VISTA blockade had superior therapeutic effects, which were associated with activation of tumor-infiltrating CD8⁺ T cells and depletion of intratumoral granulocytic myeloid-derived suppressor cells (MDSCs). Overall, these results demonstrate that RT can sensitize immunorefractory tumors to VISTA or PD-1 blockade, that this effect is enhanced by the addition of cyclophosphamide and suggest that a multipronged immunotherapeutic approach may also be required to increase the incidence of durable responses in patients with TNBC.

ARTICLE HISTORY

Received 19 August 2020
Revised 25 September 2020
Accepted 25 September 2020

KEYWORDS

C10orf54; CD8⁺ T cells; cyclophosphamide; 4T1 cells; focal radiotherapy; immunological checkpoints; immunosurveillance; MDSCs; myeloid cells; PD-1; TCGA; VSIR


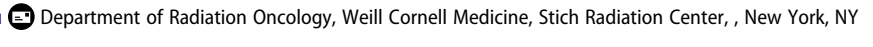
Introduction

Successful tumor rejection requires the induction of robust anticancer T-cell responses.¹ Therapeutic targeting of the immunosuppressive pathways regulated by cytotoxic T lymphocyte-associated protein 4 (CTLA4) and programmed cell death 1 (PDCD1, best known as PD-1) has been successfully implemented in the clinical management of several malignancies. However, primary and acquired resistance to immune checkpoint inhibitors (ICIs) remain an obstacle in the majority of patients.²

In breast cancer, early studies testing monoclonal antibody directed against PD-1 or its main ligand CD274 (best known as PD-L1) have shown variable but generally modest activity, which was relatively more pronounced in patients with triple-negative breast cancer (TNBC).³ Recent results from the Phase III IMpassion130 clinical trial demonstrate that the addition of the PD-L1-targeting ICI atezolizumab to nab-paclitaxel increases progression-free survival (PFS) of metastatic TNBC patients.⁴ Interim analysis also showed improved overall survival (OS) (25 mo vs. 15.5 mo) among women with PD-L1⁺ tumors (369/902, i.e., 41%). These results raise the question as to whether other cytotoxic inducers of immunogenic cell death (ICD)^{5–7} could enhance the

proportion of patients with breast cancer that respond to anti-PD-1/PD-L1 therapies. Both radiation therapy (RT) and cyclophosphamide have multiple immunomodulatory effects,^{8,9} encompassing the ability to induce ICD^{6,10,11} and boost responses to ICIs.^{12–15} In support of this notion, various clinical studies have shown a positive interaction between RT and antibodies targeting PD-1, PD-L1, or CTLA4 in patients with lung cancer.^{16–18} However, multiple co-inhibitory receptors other than PD-1 or CTLA4 have been described, potentially explaining why most patients fail to respond to the combination of RT and ICIs.¹⁹ While such receptors may offer alternative pathways of immunoevasion to developing tumors, they may also constitute potential targets for therapeutic intervention.^{20,21} In line with this possibility, multiple studies have demonstrated the advantage of simultaneously targeting distinct immunological checkpoints in preclinical tumor models.^{22–24}

V-set immunoregulatory receptor (VSIR, best known as VISTA) is a co-inhibitory receptor that shares structural resemblance with other members of the Ig domain-containing B7 family.²⁵ VISTA is constitutively expressed in the hematopoietic compartment, with the highest expression

CONTACT Silvia C. Formenti  formenti@med.cornell.edu 

 Supplemental data for this article can be accessed on the [publisher's website](#).

© 2020 The Author(s). Published with license by Taylor & Francis Group, LLC.

This is an Open Access article distributed under the terms of the Creative Commons Attribution-NonCommercial License (<http://creativecommons.org/licenses/by-nc/4.0/>), which permits unrestricted non-commercial use, distribution, and reproduction in any medium, provided the original work is properly cited.

levels found on myeloid cells. Specifically, VISTA suppresses cytokine production by antigen-presenting cells and hence their ability to drive proliferative T cell responses.²⁶ VISTA is also expressed on (and inhibits the activity of) CD4⁺ T cells,²⁷ where expression overlaps with that of PD-1 and other co-inhibitory receptors.²⁶ Studies from knock-out mice indicate that VISTA and PD-1 have distinct and non-overlapping roles in the regulation of T-cell activation, which can be therapeutically targeted to achieve a synergistic anti-tumor activity.²⁸

Here, we used mouse 4T1 mammary cancer cells as a model of rapidly metastatic and poorly immunogenic TNBC²⁹ to test the hypothesis that a multipronged therapeutic strategy including ICD inducers like RT and cyclophosphamide as well as ICIs is required for the activation of robust antitumor immune responses, capable to limit metastatic dissemination and increase survival. VISTA emerged as a promising candidate, largely in line with the notion that immunosuppressive myeloid cells have been shown to constitute a large fraction of the immunological infiltrate of human breast cancer,³⁰ they are induced by focal radiotherapy and they express high levels of VISTA.

Our data suggest that optimal therapeutic responses of immunotherapy against TNBC require a multipronged approach that leverages the direct immunostimulation of focal radiotherapy while limiting lymphoid (anti-PD-1, anti-VISTA) and myeloid (cyclophosphamide) immunosuppression. These results provide the rationale for testing VISTA blockade as a component of a multipronged immunotherapeutic approach for tumors that are insensitive to radiation and PD-1 blockade.

Materials and methods

Cells and reagents

Mouse 4T1 mammary cells were grown in DMEM supplemented with 2 mol/L *L*-glutamine, 100 U/mL penicillin, 100 µg/mL streptomycin, 25 µmol/L 2-mercaptoethanol and 10% fetal bovine serum (Invitrogen). Cells were authenticated by morphology, growth, and pattern of metastasis *in vivo* and routinely screened for *Mycoplasma spp.* contamination with the LookOut[®] Mycoplasma PCR Detection Kit (Sigma-Aldrich). The InVivoMAB mouse anti-PD-1 antibody (Clone RMP1-14) was purchased from BioXCell. The anti-VISTA antibody (Clone 13F3) was generously provided by Janssen Pharmaceuticals.

Animal experiments

Six to eight-week-old wild-type female BALB/c mice were obtained from Taconic. All *in vivo* experiments were approved by the Institutional Animal Care and Use Committee (IACUC) of Weill Cornell Medicine. Mice were subcutaneously (*s.c.*) inoculated with 0.5×10^5 4T1 cells and randomly assigned to treatment groups thirteen days later, when tumors typically achieved an average diameter of 5 mm. Focal RT was given with the Small Animal Radiation Research Platform (SARRP, from Xstrahl Ltd) in two doses of 12 Gy each on days 13 and 14 post-tumor implantation. To this aim, mice were anesthetized with isoflurane and animals

assigned to radiation were placed on a dedicated tray and positioned so that only the tumor was targeted by the radiation beam by means of a 10 × 10 mm collimator. Tumors were measured every 2–3 days until euthanasia (at experimental endpoints, when tumor exceeded 5% of body weight, or if mice showed signs of pain or distress). Perpendicular tumor diameters were obtained using a Vernier caliper and total tumor volume calculated following the common ellipsoid approach^{12,31,32} as longer diameter × shorter diameter² × $\pi/6$. Cyclophosphamide (100 mg/kg body weight) was given *i.p.* on day 9 post tumor implantation. Systemic (*i.p.*) checkpoint blockade using monoclonal antibodies targeting PD-1 (Clone RMP1-14, 200 µg/mouse) and/or VISTA (Clone 13F3, 10 mg/kg) was initiated the day after the last RT dose. In experiments evaluating the efficacy of treatment on metastatic dissemination, mice were euthanized on day 32 and excised lungs were fixed in 4% paraformaldehyde. Gross lung metastases were enumerated using a dissecting microscope by at least 3 observers, which were blinded to the treatment received by each specimen.

Flow cytometry

4T1 tumors were excised and digested with the Mouse Tumor Dissociation kit (Miltenyi Biotec) as per manufacturer's instructions, and ran on a Miltenyi gentleMACS Octo Dissociator with Heaters using pre-set program (37C_m_TDK2). The resulting cell suspensions were filtered using a 40 µm cell strainer and subjected to RBC lysis. Samples were counted and stained with the Zombie Aqua Fixable Viability Dye (BioLegend) to distinguish live cells. All samples were then incubated with purified anti-mouse CD16/32 (Fc block) prior to staining. The following anti-mouse antibodies, all purchased from BioLegend, were used for immunostaining in the indicated dilutions: CD69 APC (Clone H1.2 F3) 1:100, CD4 PE/Cy5 (Clone GK1.5) 1:100, FOXP3 Alexa Fluor 488 (Clone 150D) 1:50, CD25 APC (Clone PC61) 1:100, CD45 APC-Cy7 Clone 30-F11 (1:500), CD3 BV421 Clone 145-2 C11(1:100), CD8 FITC Clone 53-6.7 (1:100), CD11b PerCP-Cy5.5 Clone M1/70 (1:200), Ly6G Alexa Fluor 488 (Clone 1A8) 1:100, Ly6C Brilliant Violet 421 (Clone HK1.4) 1:100, CD4 PerCP-Cy5.5 Clone GK1.5 (1:100). Flow data were acquired using a MACSQuant Analyzer 10 and analyzed using FlowJo version 10.1 (Tree Star).

Ex vivo IFN γ production

0.5×10^6 cells from tumor-draining lymph nodes were cultured in RPMI 1640 medium supplemented with 10% fetal bovine serum, 2 mmol/L *L*-glutamine, 100 U/mL penicillin, 100 µg/mL streptomycin, 25 µmol/L 2-mercaptoethanol in a 48-well plate. Feeder cells were obtained from naïve BALB/c mice using 3×10^6 irradiated (12 Gy) splenocytes pre-loaded with the tumor-associated immunodominant antigen AH-1-A5 (SPSYAYHQF) or the irrelevant peptide pMCMV (YPHFMPTNL), both from Genscript, at a final concentration of 1 µg/mL. Supernatants were collected after 48 hours and secreted IFN γ was measured using the Mouse IFN-gamma Quantikine ELISA Kit (R&D Systems).

Statistical analysis

Statistical analyses were done using GraphPad Prism v. 8. To determine significant differences in tumor volumes among treatment groups, two-way ANOVA with repeated measures and Tukey correction for multiple comparisons was utilized. For in vitro experiments, ordinary one-way ANOVA with Holm-Sidak's posttest correction for samples with single pooled variance was employed to identify significant changes. Kruskal–Wallis test with Dunn's correction for multiple comparisons was used to detect significant differences in lung metastases among treatment groups. The Kaplan–Meier method was used to estimate median OS and the log cumulative hazard transformation was used to derive 95% confidence limits for median OS in each arm. Differences in OS curves were compared using log-rank (Mantel-Cox) test with correction for multiple pairwise comparisons. All reported *p* values are two-sided and statistical significance is defined as *p* < .05.

TCGA analysis

Patients with TNBC (*n* = 116) were identified in The Cancer Genome Atlas (TCGA) public database (<https://cancergenome.nih.gov/>). Differentially expressed genes (DEGs) between the *VSIR*^{high} and *VSIR*^{low} groups were determined using the LIMMA-R package.³³ Hierarchical clustering analysis was conducted using the ComplexHeatmap package, based on the Pearson distance and complete clustering method.³⁴ The MCP-counter R package and “metagene” markers were used to estimate the relative abundance of tissue-infiltrating immune cell populations.^{35,36} Functional and enrichment analysis of DEGs was performed using the ClusterProfiler.³⁷ Survival analysis was performed using the Survival and Survminer R packages, based on log-rank tests. The prognostic value of continuous variables was assessed using median cutoffs. Correlation was analyzed by the Spearman's correlation approach and visualized by using the corrplot package in R. GSEA analyses were performed using the fgsea package in R and loading gene set analysis was conducted using MSigDB gene sets H₁ from msigdb R package.³⁸ R version 3.6.0 was used for all in silico studies.

Results

Focal RT elicits local and systemic anticancer effects in the context of multiple immune checkpoint blockade

The mouse mammary carcinoma 4T1 model is a well-characterized model of cold, highly metastatic, and immunotherapy-resistant mammary tumor, mimicking the behavior of aggressive TNBC in humans.^{29,39–41} Treatment of 4T1 tumors established in syngeneic BALB/c mice with ICIs targeting CTLA4 and/or PD-1 is ineffective.²⁹ We have previously shown that RT directed to primary 4T1 tumors enables responsiveness to CTLA4- or PD-1-targeting ICI by inducing T cells that are able to reject the irradiated tumor and reduces metastatic dissemination to the lungs.^{12,42} Although mice treated with RT plus ICIs experience increased OS as compared to mice receiving ICIs alone, they ultimately succumb to disease progression, suggesting the presence of additional barriers limiting tumor rejection. One such

barrier may be represented by MDSCs, which are abundant in the 4T1 microenvironment,^{29,43} and are known to mediate robust immunosuppressive effects both mice and humans⁴⁴ prompting interest in developing therapeutic strategies to target them.⁴⁵

Since myeloid cells have been shown to express high levels of the VISTA,²⁵ we asked whether targeting VISTA could improve responses to RT and PD-1 blockade in the 4T1 model. As monotherapy, neither VISTA nor PD-1 blockade limited the progression of 4T1 tumors established in BALB/c mice (Suppl. Fig. 1A,B). Conversely, both the VISTA-targeting and the PD-1-targeting ICI significantly improved the local control of 4T1 tumors receiving 2 focal RT doses of 12 Gy each, on two consecutive days (Figure 1(a)) and reduced the number of lung metastases (Suppl. Fig. 1 C). Local tumor control rates achieved with the RT plus VISTA blockade were comparable to those observed with RT plus PD-1 blockade. However, dual VISTA/PD-1 blockade failed to further improve local or systemic tumor control rates achieved with RT plus PD-1 or VISTA blockade (Figure 1(a) and Suppl. Fig. 1 C). These results lend further support to the notion that RT can be

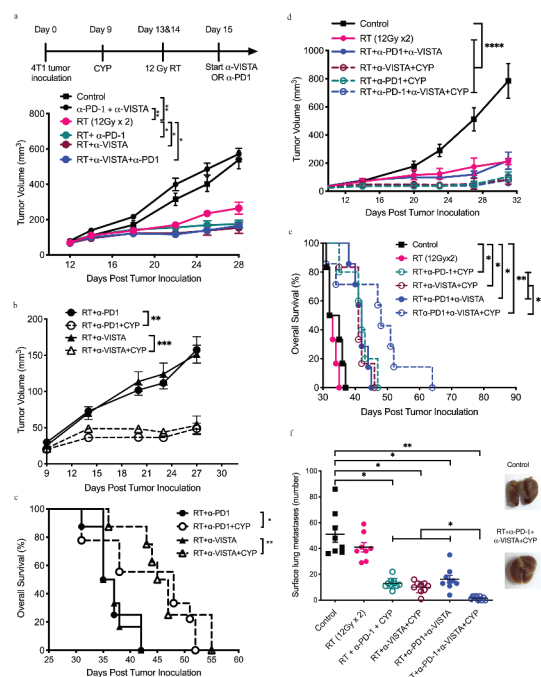


Figure 1. Anti-tumor effect of dual PD-1/VISTA blockade in 4T1 tumor-bearing mice requires radiotherapy and pre-treatment with cyclophosphamide. (a) 4T1 cells were injected s.c. at day 0 into syngeneic BALB/c mice, and treatment started when tumors reached average volume of 100mm³ (day 13). Anti-VISTA mAb 13F3 (300 μg/mouse) or PBS was given *i.p.* starting on day 13 thrice weekly for a total of 6 doses. Anti-PD-1 mAb RMP1-14 (200 μg/mouse) or PBS was given *i.p.* starting on day 13 every 3 days for a total of three doses. 4T1 tumor-bearing mice (*n* = 6–8 mice per treatment group) were randomly assigned to six treatment groups, as indicated. Tumor growth over time (**p* < .05, ***p* < .005, two-way ANOVA) (b,c) CYP (100 mg/kg *i.p.*) was given on day 9, RT and antibodies were administered as in Figure 1(a). (b) Tumor growth over time (***p* < .005, ****p* < .0005, two-way ANOVA) (c) Survival (**p* < .05, ***p* < .005, Log-rank test) (d-f) Mice (*n* = 6–8/group) were inoculated with 4T1 cells on day 0 and treated with CYP prior to RT and anti-VISTA and/or anti-PD-1 antibody administration, as described in Figure 1(a). (d) Tumor growth over time, **p* < .05, ***p* < .005, two-way ANOVA) (e) Effects of treatment on survival (**p* < .05, ***p* < .005, Log-rank test). (f) In a separate experiment, mice were euthanized on day 32 for evaluation of lung metastases. Each symbol represents an individual mouse (**p* < .05, ***p* < .005, Mann-Whitney test).

used to sensitize immunoresistant tumors to ICIs but do not suggest a benefit for dual VISTA and PD-1 blockade.

Next, we asked whether the responses obtained with RT plus VISTA blockade could be further improved by cyclophosphamide, a chemotherapeutic agent with broad immunomodulatory properties⁶ that has been successfully exploited in preclinical studies as a therapeutic partner for vaccine-based and other immunotherapeutic approaches.^{46–48} We thus tested the effect of a single low dose of cyclophosphamide (100 mg/kg) given a few days prior to RT, based on a treatment schedule that was previously shown to induce durable anti-tumor immunity along with a temporary decrease in regulatory T (T_{REG}) cells in 4T1-bearing mice treated with RT and a Toll-like receptor 7 (TLR7) agonist.⁴⁷ In our model, treatment with cyclophosphamide alone neither delayed tumor growth or OS, nor did it improve therapeutic responses to RT (Suppl. Fig. 1D,E). However, when combined with RT plus PD-1 ($p = .0014$) or VISTA ($p = .0003$) blockade cyclophosphamide significantly improved tumor control and OS. (Figure 1(b,c)).

Next, we tested a multipronged immunotherapeutic strategy involving cyclophosphamide, RT as well as PD-1- and VISTA-targeting ICIs. The effect of cyclophosphamide pre-administration on tumor control in mice treated with radiation plus dual PD-1/VISTA blockade was comparable to that achieved by radiation plus either checkpoint blockade (mean tumor volume at day 31: $103.53 \pm 12.79 \text{ mm}^3$ in cyclophosphamide plus RT plus PD-1 blockade, $82.1 \pm 12.6 \text{ mm}^3$ in cyclophosphamide plus RT plus VISTA blockade vs. $81.3 \pm 17.7 \text{ mm}^3$ in cyclophosphamide plus RT plus dual PD-1/VISTA blockade, $p = .9550$) (Figure 1(d)). However, mice treated with cyclophosphamide plus RT and dual PD-1/VISTA blockade experienced a significantly longer median OS as compared to all other mice (median survival: 48 days for cyclophosphamide plus RT plus VISTA and PD-1 blockade vs. 42 days for cyclophosphamide plus RT plus PD-1 blockade, $p = .048$; and 41 days for cyclophosphamide plus RT plus VISTA blockade, $p = .0495$.) (Figure 1(e)). Importantly, cyclophosphamide was required for survival extension, as median OS in mice treated with RT plus dual PD-1/VISTA blockade was significantly shorter (42 days, $p = .0351$).

As the survival of 4T1 tumor-bearing mice is mainly dictated by metastatic spread to the lungs,³⁹ we set to evaluate metastatic lung burden prior to overt symptoms of respiratory distress. Mice treated with cyclophosphamide plus RT and dual PD-1/VISTA blockade had significantly fewer lung metastases as compared to all other groups, with one-third of these animals free of metastases at 32 days after tumor inoculation (mean number of metastases: 13.1 ± 1.2 for cyclophosphamide plus RT plus PD-1 blockade, 10.11 ± 1.4 for cyclophosphamide plus RT plus VISTA blockade vs. 1.7 ± 0.47 for cyclophosphamide plus RT and dual PD-1/VISTA blockade, $p = .0002$) (figure 1(f)).

We further tested whether the timing of cyclophosphamide administration could affect its beneficial effects on systemic tumor control. Machiels and coworkers had previously demonstrated that optimal antitumor immune responses were achieved when cyclophosphamide was given a few days before a GM-CSF-secreting whole-cell vaccine.⁴⁸ On the other hand, improved tumor responses to RT have been demonstrated when cyclophosphamide was given concurrently to irradiation.⁴⁹ Thus, we

compared the administration of cyclophosphamide 4 days before RT (day 9) vs. concurrent with the first RT dose (day 13) (Suppl. Fig. 2A). No difference in efficacy (neither on tumor growth nor on metastatic dissemination) could be observed when cyclophosphamide was delivered according to different schedules in the context of RT plus dual PD-1/VISTA blockade (Suppl. Fig. 2B, C). Overall, these findings support an essential role for low-dose cyclophosphamide to maximize the ability of RT plus dual PD-1/VISTA to control the progression and metastatic dissemination of 4T1 tumors.

Cyclophosphamide in combination with RT and dual PD-1/VISTA blockade enables the priming of tumor-specific CD8⁺ T cells coupled with MDSC depletion

To understand the mechanisms underlying the improved control of lung metastases in 4T1 tumor-bearing mice treated with cyclophosphamide plus RT and dual PD-1/VISTA blockade, we analyzed the tumor immune infiltrate at day 18, 3 days after administration of the first ICI dose (Figure 2(a)). The flow cytometry-assisted analysis of immune cells isolated from 4T1 tumors demonstrated that RT was required, but not sufficient, to drive robust tumor infiltration by CD8⁺ T cells. Indeed, a significant increase in intratumoral CD8⁺ T cells was observed in animals treated with RT plus PD-1 blockade ($p = .022$) or RT plus VISTA blockade ($p = .024$), but not RT alone. The combination of cyclophosphamide plus RT and dual PD-1/VISTA blockade induced the largest augmentation in tumor-infiltrating CD8⁺ T cells, which expressed increased levels of the activation marker CD69 (Figure 2(b,c)). The fraction of tumor-infiltrating CD8⁺ T cells expressing high levels of PD-1, which is a marker terminally activated/exhausted T cells,⁵⁰ was reduced in mice treated with cyclophosphamide plus RT and single or dual VISTA/PD-1 blockade, as well as mice treated with RT plus dual VISTA/PD-1 blockade in the absence of cyclophosphamide (Figure 2(d)). We next investigated tumor-specific CD8⁺ T cell responses in tumor-draining lymph nodes. Notably, interferon gamma (IFN γ , best known as IFN- γ) secretion by tumor-infiltrating CD8⁺ T cells exposed to the CD8 epitope AH-1-A5, which is derived from the envelope of an endogenous retrovirus expressed by 4T1 cells,^{51,52} was markedly increased only in mice treated with cyclophosphamide plus RT and dual PD-1/VISTA blockade ($p < .005$) (Figure 2(e)). Thus, in the 4T1 model of TNBC, only a multipronged immunotherapeutic strategy comprising cyclophosphamide, RT and two ICIs elicits abundant tumor infiltration by activated CD8⁺ T cells plus robust priming of tumor-specific immunity.

Analysis of the CD4 compartment revealed no significant changes in total CD4⁺ T cells in any of the treatment groups (figure 2(f)). Similarly, the proportion of T_{REG} cells, which constituted ~70% of all CD4⁺ T-cells in untreated 4T1 tumors, was not significantly altered by treatment (Figure 2(g)). However, activated CD4⁺ effectors, identified by interleukin 2 receptor subunit alpha (IL2RA, best known as CD25) expression and forkhead box P3 (FOXP3) lack of expression, were increased in the tumors of mice treated with cyclophosphamide plus RT and PD-1, VISTA or dual PD-1/VISTA blockade (Figure 2(h)). Cyclophosphamide has previously been shown to temporarily decrease T_{REG} cells.^{47,48} As we failed to observe such a decrease in intratumoral T_{REG} cells in mice received cyclophosphamide

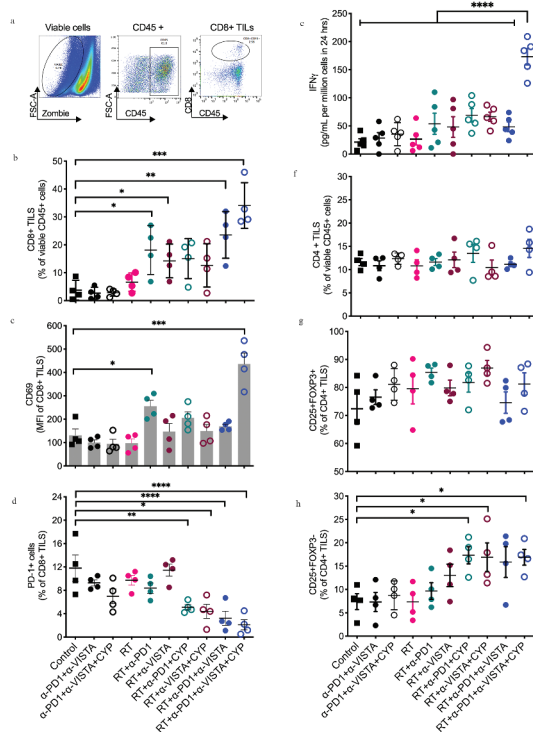


Figure 2. Changes in tumor infiltration by CD8⁺ T cells induced following the different treatments. 4T1 tumor-bearing mice were treated as described in Figure 1(a). On day 18 post 4T1 cell injection, tumors were excised and digested and single-cell suspensions analyzed by flow cytometry. (a) A multi-step gating strategy was employed to identify CD8⁺ TILs in dissociated tumors. Positive populations were identified based on negative staining on fluorescence-minus-one (FMO) controls. (b) Percentage of CD8⁺ T cell infiltration. (c) CD69 expression in CD8⁺ T cells and (d) percentage of CD8⁺ TILs expressing PD-1. (b-d, **p* < .05, ***p* < .005, ****p* < .0005, *****p* < .0001, one-way ANOVA). (e) Effect of treatment on tumor-specific IFN-γ response in tumor-draining lymph nodes. Dissociated cell suspensions were incubated with peptides (tumor-specific epitope AH-1-A5) or irrelevant peptide pMCMV and IFN-γ production measured 48 hours later by ELISA. Each symbol represents the response of an individual mouse to tumor epitope AH-1-A5 after subtraction of the background response to pMCMV (*****p* < .0005, one-way ANOVA). (f) Percentage of CD4⁺ T cell infiltration. (g) Proportion of CD4⁺CD25⁺FOXP3⁺ regulatory T (T_{REG}) cells in the CD4 compartment. (h) Expression of CD25 among effector CD4⁺ T cells. (**p* < .05, one-way ANOVA).

for 9 days (data not shown), we asked whether T_{REG} cells could have been depleted earlier, shortly after cyclophosphamide administration. To address this question, T_{REG} cells were analyzed in the spleen and tumor of mice treated with cyclophosphamide and/or RT at different time points: (1) 3 days after cyclophosphamide administration (day 12), (2) at completion of RT (day 15), and (3) at day 20 (Supp. Fig 2D). This analysis revealed a mild but significant decrease in T_{REG} cells in both the spleen and tumor of mice treated with RT plus cyclophosphamide at day 15, but T_{REG} cells quickly rebounded to baseline levels by day 20 (Suppl. Fig. 2E,F).

To gain more insights into the mechanisms underlying the development of antitumor immunity in mice treated with cyclophosphamide plus RT and dual PD-1/VISTA blockade, we next analyzed MDSCs. Differential expression of lymphocyte antigen 6 complex, locus G (Ly6G) and lymphocyte antigen 6 complex, locus C (Ly6C) on intratumoral CD11b⁺ cells defines the two major MDSC subsets: monocytic MDSCs (mMDSCs, Ly6G⁻Ly6C^{hi}) and granulocytic MDSCs (gMDSCs, Ly6G⁺Ly6C^{low}).^{53,54} Both MDSC subsets infiltrating 4T1 tumors

expressed comparable levels of VISTA (Figure 3(a)). In untreated mice, CD11b⁺ myeloid cells comprised approximately 55% of all tumor-infiltrating CD45⁺ cells (Figure 3(b)), ~40% of which were granulocytic MDSCs (Figure 3(c,d)). In the absence of RT and regardless of cyclophosphamide treatment, dual PD-1/VISTA blockade did not alter the abundance of tumor-infiltrating CD11b⁺ cells. Similarly, RT employed as a standalone treatment did not significantly impact tumor infiltration by CD11b⁺ myeloid cells (Figure 3(b)). Conversely, RT combined with VISTA (but not PD-1) blockade led to a significant decrease in tumor-infiltrating CD11b⁺ cells (Figure 3(b)), particularly in the granulocytic MDSC compartment (Figure 3(c)). Addition of cyclophosphamide and a PD-1-targeting ICI to RT plus VISTA blockade did not further decrease the proportion of tumor-infiltrating gMDSCs. Finally, also in the absence of VISTA blockade, the combination of cyclophosphamide with RT and PD-1 blockade significantly reduced CD11b⁺ myeloid cells as compared to control conditions (Figure 3(b)). Of note, RT was critical to achieve gMDSC depletion even in the context of cyclophosphamide plus dual PD-1/VISTA blockade (mean %: 53.55 ± 2.44 for cyclophosphamide plus dual PD-1/VISTA blockade vs. 19.9 ± 3.18 for cyclophosphamide plus RT and dual PD-1/VISTA blockade, *p* = .0001), suggesting that RT induces key changes in the tumor microenvironment that are required for VISTA blockade to deplete gMDSCs.

Impact of VISTA on the immune infiltrate of breast cancer patients

To investigate the translational value of our findings, we took advantage of The Cancer Genome Atlas (TCGA) public patient dataset, which contains annotated bulk transcriptomic data for 116 patients with immunohistochemistry-confirmed TNBC. First, we interrogated whether VISTA expression levels would

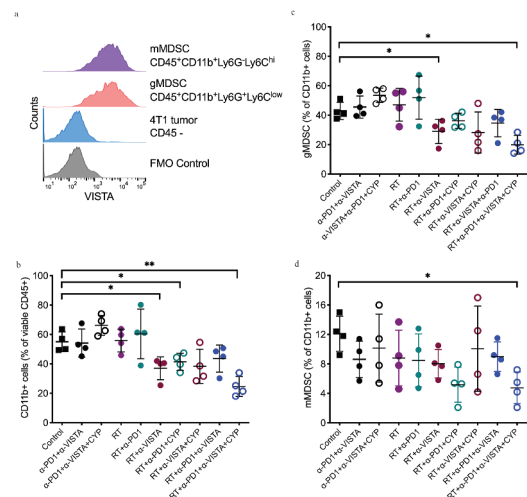


Figure 3. Changes in tumor infiltration by MDSC induced following the different treatments. 4T1 tumor-bearing mice were treated as described in Figure 1A. On day 18 post 4T1 cell inoculation, tumors were excised and digested and single-cell suspensions analyzed by flow cytometry. Samples were gated on viable CD45⁺ cells. (a) Representative histograms show surface expression of VISTA in monocytic and granulocytic MDSCs. Gates were drawn based on negative staining of fluorescence-minus-one (FMO) control. (b) Percentage of CD11b⁺ cells in 4T1 tumors of mice in each treatment group. (c) Percentage of granulocytic MDSCs among CD11b⁺ cells. (d) Percentage of monocytic MDSCs among CD11b⁺ cells. (**p* < .05, ***p* < .005, one-way ANOVA).

be indicative of increased immune infiltration by T cells, based on Spearman correlation on genes the encode phenotypic markers preferentially (although not exclusively) expressed by these immune effector cells. We found that *VSIR* levels positively correlate with general markers of the T cell compartment (e.g., *CD3E*), with markers of specific T cell populations (e.g., *CD4*, *CD8A*, *FOXP3*), as well as with co-inhibitory T cell receptors (e.g., *CTLA4*, *HAVCR2*, *LAG3*, *PDCD1*) (Figure 4(a)). Based on our previous observations in the ovarian setting,²¹ we postulated that such an immunological configuration would be associated with improved OS. However, *VSIR* levels did not influence the OS of patients with TNBC from the TCGA, neither when patients were stratified based on median *VSIR* levels (Figure 4(b)), nor when *VSIR* was assessed as a continuous variable (HR: 1.34; 95% CI: 0.84;2.15; $p = .22$).

We thus hypothesized that other immunological features of the tumor microenvironment of patients with TNBC from the TCGA could be relevant. We, therefore, tested the relative abundance of multiple immune cell subsets in patients with higher-than-median (*VSIR*^{high}) versus lower-than-median (*VSIR*^{low}) *VSIR* levels by harnessing the MCPcounter R package, which is based on gene signatures that identify specific immune cell populations.³⁵ As compared to their *VSIR*^{low} counterparts, *VSIR*^{high} tumors were enriched not only in lymphoid cells encompassing T cells, CD8⁺ T cells, cytotoxic lymphocytes, T_{REG} cells, B cells, and NK cells (largely replicating the results of our Spearman correlation analysis), but also in cells from the monocytic lineage, myeloid dendritic cells, MDSCs, macrophages, and neutrophils (Figure 4(c)). Consistent with these findings, the unsupervised hierarchical clustering of patients with TNBC from the TCGA based on the 400 most differentially expressed genes between *VSIR*^{high} and *VSIR*^{low} tumors, identified two major patient clusters that were almost precisely determined by *VSIR* status (Figure 4(d)), and were largely defined by signatures of immunological competence (*VSIR*^{high} vs. *VSIR*^{low}) (Figure 4(e)). Thus, *VSIR*^{high} TNBCs stand out as tumors with a complex lymphoid and myeloid infiltrate.

We next tested whether immunosuppressive features of the myeloid immune infiltrate would correlate with *VSIR* levels in this patient subset. We found that *VSIR* levels correlate (to variable degrees) with the abundance of *TGFB1* and *IL10* (coding for two cytokines with robust immunosuppressive activity), *ENTPD1* and *4NTE* (which code for two ectonucleotidases involved in the generation of the immunoregulatory metabolite adenosine),^{55,56} *IDO1* (encoding an intracellular enzyme involved in the degradation of tryptophan, which is required for optimal T cell activity, and the synthesis of kynurenine, which is immunosuppressive)^{57,58} as well as *CD38* (which codes for another extracellular enzyme with immunoregulatory activity)⁵⁹ (Figure 4(f)). In line with this notion, *VSIR*^{high} TNBCs significantly differed from their *VSIR*^{low} counterparts in the relative abundance of each of these transcripts taken individually and in association, conveying a global signature of myeloid immunosuppression (Figure 4(g)).

With the caution imposed by the transcriptomic analysis of a single patient cohort, the immunological signature we documented in *VSIR*^{high} TNBCs lend further support to our preclinical findings indicating that optimal therapeutic response to

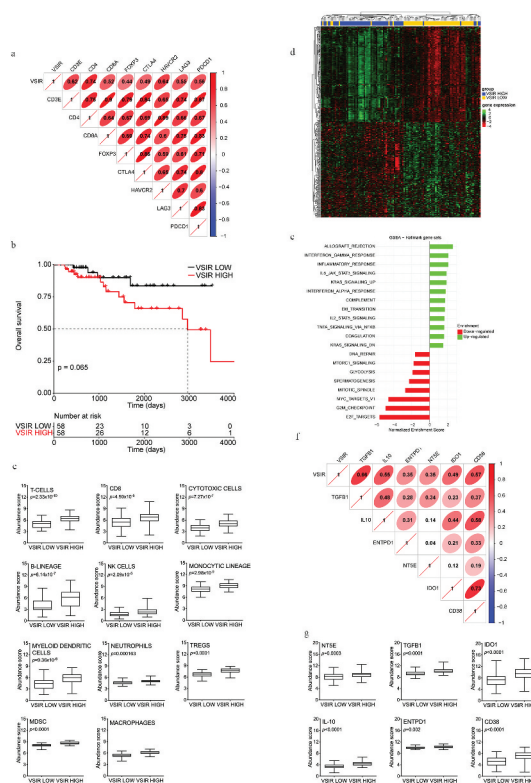


Figure 4. VISTA expression in human TNBC correlates with immunoregulatory gene signature. (a) Correlation between *VSIR* gene expression and expression levels of eight selected immune genes in TNBC (TCGA-BRCA) cohort. The correlation coefficient is displayed. (b) Overall survival of 116 TNBC patients from the TCGA-BRCA database stratified based on median expression level of *VSIR* gene. (c) Relative expression levels of gene sets associated with T-cells, CD8 cells, Cytotoxic cells, B cells, natural killer (NK) cells, TH1 cells, monocytes, myeloid dendritic cells, neutrophils, regulatory T (TREGS) cells, myeloid-derived suppressor cells (MDSC) and macrophages between *VSIR* LOW and *VSIR* HIGH patients from TNBC (TCGA-BRCA) cohort. Box plots: lower quartile, median, upper quartile; whiskers, minimum, maximum. (d) Unsupervised hierarchical clustering of differentially expressed genes that were significantly changed (adjusted p -value < 0.05) in *VSIR* HIGH versus *VSIR* LOW patients in TNBC (TCGA-BRCA) cohort. (e) GSEA Bar plot for enriched GSEA HALLMARK categories. Only categories with adjusted $p < .05$ were considered significant. Bar plot depicting the normalized enrichment scores of the most positively (green) and negatively (red) enriched categories in *VSIR* HIGH patients. (f) Correlation between *VSIR* gene expression and expression levels of immunoregulatory genes for TNBC cohort in the TCGA-BRCA dataset. The correlation coefficient is displayed. (g) Relative expression levels of immunoregulatory genes between *VSIR* LOW and *VSIR* HIGH group of patients from TNBC (TCGA-BRCA) cohort. Box plots: lower quartile, median, upper quartile; whiskers, minimum, maximum.

radiation therapy plus *VSIR* inhibitors may require not only immune checkpoint blockers to offset immunosuppression in the lymphoid compartment, but also strategies to target myeloid immunosuppression (cyclophosphamide).

Discussion

The success of ICIs that target CTLA4 and PD-1 for the management of an ever-growing list of malignancies underlies the key relevance of immunosuppressive pathways that prevent T cells from effectively recognizing and killing their neoplastic counterparts.⁶⁰ However, while durable responses to ICI-based immunotherapy have been documented in a fraction of patients with solid tumors, most patients fail to respond to ICI when employed as single agents. Efforts to increase response rate by simultaneously blocking the two co-

inhibitory receptors CTLA4 and PD-1 have been successful in patients with melanoma and lung cancer, but at the expense of increased toxicity.^{61–63} In addition, DNA-damaging agents with immunostimulatory effects, such as focal RT, have been shown to synergize with ICIs in some patient populations.^{17,18,64} These findings demonstrate that combining multiple immunotherapies with non-overlapping mechanisms of action may constitute a valuable strategy to increase response rate to ICI-based immunotherapy.

PD-1 and VISTA regulate immune responses via non-overlapping pathways, and the concurrent targeting of PD-1 and VISTA has been shown to improve the control of mouse CT26 colorectal carcinomas as compared to either agent employed as monotherapy.²⁸ However, we found that 4T1 tumors are refractory to VISTA blockade alone as well as to dual PD-1/VISTA blockade (**Supp Fig. 1**). Prior work by Le Mercier and colleagues has demonstrated that antibody-mediated VISTA blockade limits the growth of various mouse tumors, at least in part by depleting MDSCs.⁶⁵ In our study, we used the same antibody clone used by Le Mercier and collaborators,⁶⁵ pointing to the highly immunosuppressive microenvironment established by growing 4T1 tumors as to the reason for limited monotherapeutic activity. Consistent with this notion, VISTA blockade was able to deplete MDSCs in the microenvironment of 4T1 tumors only when given with RT (**Figure 3**).

Moreover, VISTA administration significantly improved the control of irradiated 4T1 tumors and metastatic dissemination, an effect that was comparable to the PD-1 blockade. Dual PD-1/VISTA blockade failed to further improve tumor control in this setting (**Figure 1**). However, when low-dose cyclophosphamide was administered before RT, we observed a significant improvement in tumor control and OS in mice treated with RT plus PD-1 or VISTA blockade, and that combination of all four therapies (cyclophosphamide, RT, PD-1 blockade, VISTA blockade) further extended OS resulting in almost complete control of lung metastases, independently of the time of administration of cyclophosphamide (**Figure 1** and Suppl. Fig. 2).

In the absence of immunotherapy, cyclophosphamide did not increase RT-mediated tumor control (Suppl. Fig. 1), suggesting a role for the immunomodulatory effects of cyclophosphamide in the improved tumor responses enabled by ICIs. Such effects have generally been linked to the depletion of intratumoral T_{REG} cells, which in rodents are more sensitive to cyclophosphamide than conventional T cells.⁶⁶ There was a small and temporary reduction in T_{REG} cells in the spleen and tumor of 4T1 tumor-bearing mice treated with RT and cyclophosphamide, but T_{REG} cells represented the majority of the CD4 compartment in tumors exposed to various combinations of RT and ICIs regardless of cyclophosphamide (**Figure 2** and Suppl. Fig. 2). Thus, it is unlikely that the ability of cyclophosphamide to dramatically enhance the priming of tumor-specific CD8⁺ T cells in mice treated with RT and dual PD-1/VISTA blockade (**Figure 2**) originates from T_{REG} cell depletion. Cyclophosphamide has also been shown to promote the activation of cytotoxic CD8⁺ T cells and T_{H1}/T_{H17} polarization in CD4⁺ T cells,⁸ at least in part linked to the ability of cyclophosphamide to reshape the intestinal microbiota.⁶⁷ Thus, it is conceivable that the improved anti-tumor T cell responses observed in mice treated with cyclophosphamide plus RT and dual PD-1/VISTA blockade may

reflect at least some degree of systemic immunomodulation by cyclophosphamide⁶⁸ coupled to (1) MDSC depletion by cyclophosphamide and (2) de-repression of the effector phase of the immune response in the tumor microenvironment by VISTA and PD-1 blockade.

With the caveats associated with a retrospective transcriptomic study based on a relatively small patient cohort, our preclinical findings are supported by the fact that the microenvironment of patients with TNBC from the TCGA database containing high *VSIR* levels is enriched in gene signatures pointing to a robust myeloid immunosuppression (**Figure 4**). Moreover, CD68⁺ macrophages have recently been identified as an important reservoir of VISTA-expressing cells in prostate and pancreatic tumors,^{69,70} suggesting a key role for VISTA in the myeloid tumor microenvironment. Of note, RT can drive robust tumor infiltration by myeloid cells, as shown by a study in non-metastatic prostate cancer patients,⁷¹ and multiple preclinical work suggesting that RT generates a broad and complex effect on recruitment, removal, reorganization, repolarization and/or representation of tumor-infiltrating myeloid cells.^{72,73} In prostate tumors, treatment with fractionated low-dose RT led to elevated levels of macrophage colony-stimulating factor 1 (CSF1), a key cytokine driving the systemic accumulation of MDSCs.⁷⁴ In this context, RT-induced DNA damage was shown to mediate the nuclear translocation of ABL proto-oncogene 1, non-receptor tyrosine kinase (ABL1), and consequent *Csf1* transactivation. On the other hand, indolent type I interferon secretion by RT has been implicated in MDSC recruitment via C-C motif chemokine receptor 2 (CCR2),⁷⁵ which not only supports T_{REG} infiltration upon RT but also has been proposed to represent a biomarker for cyclophosphamide sensitivity.^{76,77} Most importantly, selective targeting of these axes, either by small molecule inhibitors of the CSF1 receptor or CCR2 antagonists, has defined a new therapeutic partnership to increase patient response to RT. Our study suggests that VISTA blockade stands out as an additional pathway through which the detrimental effects of myeloid (and potentially T_{REG}) cell accumulation driven by RT can be overcome.

In conclusion, our data suggest that the immunological rejection of tumors that are resistant to ICIs may require treatments that act at multiple levels, encompassing not only the robust activation of ICD (and hence an increased availability of tumor-associated antigens and danger signals), as effectively elicited by RT, but also the neutralization of immunosuppressive circuitries involving lymphoid and myeloid compartments, as mediated by multiple ICIs and cyclophosphamide, respectively. Moreover, these findings suggest that tumor types with prominent MDSC-dependent immunosuppression may benefit from combinatorial therapies that also target this compartment. Additional studies are required to translate these observations into clinical trials.

Disclosure of Potential Conflicts of Interest

M.H. and J.F. are full-time employees of Sotio. L.G. declares research funding from Lytix, and Phosphatin, and speaker and/or advisory honoraria from Boehringer Ingelheim, Astra Zeneca, OmniSEQ, The Longevity Labs, Inzen, the Luke Heller TECPR2 Foundation. S.D. has received prior honorarium for consulting from AstraZeneca, AbbVie, Lytix Biopharma,

EMD Serono, Eisai Inc., Cytune Pharma, Regeneron, and research grants from Nanobiotix, and Lytix Biopharma. S.C.F. has received prior honorarium for consulting/speaker from AstraZeneca, Merck, Regeneron, Bayer, Serono, and research funding from Varian, Merck, Bristol Meyer Squibb. All other authors have no conflicts of interests to disclose. As per standard operations at *Oncoimmunology*, LG has been excluded from all steps of editorial evaluation of the present article.

Authors contributions

Concept and design: K.A.P., S.D., S.C.F. Data acquisition: K.A.P., C.D., J.F., M.H. Data analysis and interpretation: K.A.P., M.H., J.F., L.G., S.D. Writing and/or review of manuscript: K.A.P., L.G., S.D., S.C.F. Support and infrastructure: J.F., S.C.F. Approval of the manuscript: All authors.

References

- Galluzzi L, Chan TA, Kroemer G, Wolchok JD, López-Soto A. The hallmarks of successful anticancer immunotherapy. *Sci Transl Med.* 2018;10:1–14.
- Sharma P, Hu-Lieskovan S, Wargo JA, Ribas A. Primary, adaptive, and acquired resistance to cancer immunotherapy. *Cell.* 2017;168:707–723.
- Emens LA. Breast cancer immunotherapy: facts and hopes. *Clin Cancer Res.* 2018;24:511–520.
- Schmid P, Adams S, Rugo HS, Schneeweiss A, Barrios CH, Iwata H, Diéras V, Hegg R, Im SA, Shaw Wright G, et al. Atezolizumab and nab-paclitaxel in advanced triple-negative breast cancer. *N Engl J Med.* 2018;379:2108–2121.
- Ma Y, Kepp O, Ghiringhelli F, Apetoh L, Aymeric L, Locher C, Tesniere A, Martins I, Ly A, Haynes NM, et al. Chemotherapy and radiotherapy: cryptic anticancer vaccines. *Semin Immunol.* 2010;22:113–124.
- Galluzzi L, Vitale I, Warren S, Adjemian S, Agostinis P, Martinez AB, Chan TA, Coukos G, Demaria S, Deutsch E, et al. Consensus guidelines for the definition, detection and interpretation of immunogenic cell death. *J Immunother Cancer.* 2020;8:e000337.
- Rodriguez-Ruiz ME, Vitale I, Harrington KJ, Melero I, Galluzzi L. Immunological impact of cell death signaling driven by radiation on the tumor microenvironment. *Nat Immunol.* 2020;21:120–134.
- Sistigu A, Viaud S, Chaput N, Bracci L, Proietti E, Zitvogel L. Immunomodulatory effects of cyclophosphamide and implementations for vaccine design. *Semin Immunopathol.* 2011;33:369–383.
- Demaria S, Golden EB, Formenti SC. Role of local radiation therapy in cancer immunotherapy. *JAMA Oncol.* 2015;1:1325–1332.
- Golden EB, Frances D, Pellicciotta I, Demaria S, Helen Barcellos-Hoff M, Formenti SC. Radiation fosters dose-dependent and chemotherapy-induced immunogenic cell death. *Oncoimmunology.* 2014;3:e28518.
- Rodriguez-Ruiz ME, Buque A, Hensler M, Chen J, Bloy N, Petroni G, Sato A, Yamazaki T, Fucikova J, Galluzzi L. Apoptotic caspases inhibit abscopal responses to radiation and identify a new prognostic biomarker for breast cancer patients. *Oncoimmunology.* 2019;8:e1655964.
- Demaria S, Kawashima N, Yang AM, Devitt ML, Babb JS, Allison JP, Formenti SC. Immune-mediated inhibition of metastases after treatment with local radiation and CTLA-4 blockade in a mouse model of breast cancer. *Clin Cancer Res.* 2005;11:728–734.
- Deng L, Liang H, Burnette B, Beckett M, Darga T, Weichselbaum RR, Fu YX. Irradiation and anti-PD-L1 treatment synergistically promote antitumor immunity in mice. *J Clin Invest.* 2014;124:687–695.
- Dovedi SJ, Adlard AL, Lipowska-Bhalla G, McKenna C, Jones S, Cheadle EJ, Stratford IJ, Poon E, Morrow M, Stewart R, et al. Acquired resistance to fractionated radiotherapy can be overcome by concurrent PD-L1 blockade. *Cancer Res.* 2014;74:5458–5468.
- Pilonés KA, Vanpouille-Box C, Demaria S. Combination of radiotherapy and immune checkpoint inhibitors. *Semin Radiat Oncol.* 2015;25:28–33.
- Shaverdian N, Lisberg AE, Bornazyan K, Veruttipong D, Goldman JW, Formenti SC, Garon EB, Lee P. Previous radiotherapy and the clinical activity and toxicity of pembrolizumab in the treatment of non-small-cell lung cancer: a secondary analysis of the KEYNOTE-001 phase I trial. *Lancet Oncol.* 2017;18:895–903.
- Antonia SJ, Villegas A, Daniel D, Vicente D, Murakami S, Hui R, Yokoi T, Chiappori A, Lee KH, de Wit M, et al. Durvalumab after chemoradiotherapy in stage III non-small-cell lung cancer. *N Engl J Med.* 2017;377:1919–1929.
- Formenti SC, Rudqvist NP, Golden E, Cooper B, Wennerberg E, Lhuillier C, Vanpouille-Box C, Friedman K, Ferrari de Andrade L, Wucherpfennig KW, et al. Radiotherapy induces responses of lung cancer to CTLA-4 blockade. *Nat Med.* 2018;24:1845–1851.
- Sharma P, Allison JP. Dissecting the mechanisms of immune checkpoint therapy. *Nat Rev Immunol.* 2020;20:75–76.
- Zarour HM. Reversing T-cell Dysfunction and Exhaustion in Cancer. *Clin Cancer Res.* 2016;22:1856–1864.
- Fucikova J, Rakova J, Hensler M, Kasikova L, Belicova L, Hladikova K, Truxova I, Skapa P, Laco J, Pecen L, et al. TIM-3 dictates functional orientation of the immune infiltrate in ovarian cancer. *Clin Cancer Res.* 2019;25:4820–4831.
- Vanpouille-Box C, Formenti SC. Dual transforming growth factor- β and programmed death-1 blockade: a strategy for immune-excluded tumors? *Trends Immunol.* 2018;39:435–437.
- Tauriello DVF, Palomo-Ponce S, Stork D, Berenguer-Llgero A, Badiarmentol J, Iglesias M, Sevillano M, Ibiza S, Cañellas A, Hernandez-Momblona X, et al. TGF β drives immune evasion in genetically reconstituted colon cancer metastasis. *Nature.* 2018;554:538–543.
- Mariathasan S, Turley SJ, Nickles D, Castiglioni A, Yuen K, Wang Y, Kadel EE III, Koepfen H, Astarita JL, Cubas R, et al. TGF β attenuates tumour response to PD-L1 blockade by contributing to exclusion of T cells. *Nature.* 2018;554:544–548.
- Nowak EC, Lines JL, Varn FS, Deng J, Sarde A, Mabaera R, Kuta A, Le Mercier I, Cheng C, Noelle RJ. Immunoregulatory functions of VISTA. *Immunol Rev.* 2017;276:66–79.
- Wang L, Rubinstein R, Lines JL, Wasiuk A, Ahonen C, Guo Y, Lu LF, Gondek D, Wang Y, Fava RA, et al. VISTA, a novel mouse Ig superfamily ligand that negatively regulates T cell responses. *J Exp Med.* 2011;208:577–592.
- Flies DB, Han X, Higuchi T, Zheng L, Sun J, Ye JJ, Chen L. Coinhibitory receptor PD-1H preferentially suppresses CD4 $^+$ T cell-mediated immunity. *J Clin Invest.* 2014;124:1966–1975.
- Liu J, Yuan Y, Chen W, Putra J, Suriawinata AA, Schenk AD, Miller HE, Guleria I, Barth RJ, Huang YH, et al. Immune-checkpoint proteins VISTA and PD-1 nonredundantly regulate murine T-cell responses. *Proc Natl Acad Sci U S A.* 2015;112:6682–6687.
- Mosely SI, Prime JE, Sainson RC, Koopmann JO, Wang DY, Greenawalt DM, Ahdesmaki MJ, Leyland R, Mullins S, Pacelli L, et al. Rational selection of syngeneic preclinical tumor models for immunotherapeutic drug discovery. *Cancer Immunol Res.* 2017;5:29–41.
- Markowitz J, Wesolowski R, Papenfuss T, Brooks TR, Carson WE 3rd. Myeloid-derived suppressor cells in breast cancer. *Breast Cancer Res Treat.* 2013;140:13–21.
- Pilonés KA, Charpentier M, Garcia-Martinez E, Daviaud C, Kraynak J, Aryankalayil J, Formenti SC, Demaria S. Radiotherapy cooperates with IL15 to induce antitumor immune responses. *Cancer Immunol Res.* 2020;8:1054–1063.
- Tomayko MM, Reynolds CP. Determination of subcutaneous tumor size in athymic (nude) mice. *Cancer Chemother Pharmacol.* 1989;24:148–154.
- Ritchie ME, Phipson B, Wu D, Hu Y, Law CW, Shi W, Smyth GK. limma powers differential expression analyses for RNA-sequencing and microarray studies. *Nucleic Acids Res.* 2015;43:e47.
- Gu Z, Eils R, Schlesner M. Complex heatmaps reveal patterns and correlations in multidimensional genomic data. *Bioinformatics.* 2016;32:2847–2849.
- Becht E, Giraldo NA, Lacroix L, Buttard B, Elarouci N, Petitprez F, Selves J, Laurent-Puig P, Sautès-Fridman C, Fridman WH, et al. Estimating the population abundance of tissue-infiltrating immune and

- stromal cell populations using gene expression. *Genome Biol.* **2016**;17:218.
36. Angelova M, Charoentong P, Hackl H, Fischer ML, Snajder R, Krogsdam AM, Waldner MJ, Bindea G, Mlecnik B, Galon J, et al. Characterization of the immunophenotypes and antigenomes of colorectal cancers reveals distinct tumor escape mechanisms and novel targets for immunotherapy. *Genome Biol.* **2015**;16:64.
 37. Yu G, Wang LG, Han Y, He QY. clusterProfiler: an R package for comparing biological themes among gene clusters. *OMICS.* **2012**;16:284–287.
 38. Korotkevich G, Sukhov V, Sergushichev A. Fast gene set enrichment analysis. *bioRxiv.* **2019.** 060012.
 39. Pulaski BA, Ostrand-Rosenberg S. Mouse 4T1 breast tumor model. *Curr Protoc Immunol.* Chapter 20: Unit20.2. **2001.**
 40. Aslakson CJ, Miller FR. Selective events in the metastatic process defined by analysis of the sequential dissemination of subpopulations of a mouse mammary tumor. *Cancer Res.* **1992**;52:1399–1405.
 41. Savas P, Salgado R, Denkert C, Sotiriou C, Darcy PK, Smyth MJ, Loi S. Clinical relevance of host immunity in breast cancer: from TILs to the clinic. *Nat Rev Clin Oncol.* **2016**;13:228–241.
 42. Vanpouille-Box C, Diamond JM, Pilonis KA, Zavadij J, Babb JS, Formenti SC, Barcellos-Hoff MH, Demaria S. TGF β is a master regulator of radiation therapy-induced antitumor immunity. *Cancer Res.* **2015**;75:2232–2242.
 43. Sinha P, Clements VK, Bunt SK, Albelda SM, Ostrand-Rosenberg S. Cross-talk between myeloid-derived suppressor cells and macrophages subverts tumor immunity toward a type 2 response. *J Immunol.* **2007**;179:977–983.
 44. Gabrilovich DI, Nagaraj S. Myeloid-derived suppressor cells as regulators of the immune system. *Nat Rev Immunol.* **2009**;9:162–174.
 45. Liu Y, Wei G, Cheng WA, Dong Z, Sun H, Lee VY, Cha SC, Smith DL, Kwak LW, Qin H. Targeting myeloid-derived suppressor cells for cancer immunotherapy. *Cancer Immunol Immunother.* **2018**;67:1181–1195.
 46. Taieb J, Chaput N, Schartz N, Roux S, Novault S, Ménard C, Ghiringhelli F, Terme M, Carpentier AF, Darrasse-Jeze G, et al. Chemoimmunotherapy of tumors: cyclophosphamide synergizes with exosome based vaccines. *J Immunol.* **2006**;176:2722–2729.
 47. Dewan MZ, Vanpouille-Box C, Kawashima N, DiNapoli S, Babb JS, Formenti SC, Adams S, Demaria S. Synergy of topical toll-like receptor 7 agonist with radiation and low-dose cyclophosphamide in a mouse model of cutaneous breast cancer. *Clin Cancer Res.* **2012**;18:6668–6678.
 48. Machiels JP, Reilly RT, Emens LA, Ercolini AM, Lei RY, Weintraub D, Okoye FI, Jaffee EM. Cyclophosphamide, doxorubicin, and paclitaxel enhance the antitumor immune response of granulocyte/macrophage-colony stimulating factor-secreting whole-cell vaccines in HER-2/neu tolerized mice. *Cancer Res.* **2001**;61:3689–3697.
 49. Zachariae C, Overgaard J. Interactions of radiation, cyclophosphamide and nimorazole in a C3H mammary carcinoma in vivo. *Int J Radiat Oncol Biol Phys.* **1986**;12:1445–1448.
 50. Thommen DS, Schumacher TN. T cell dysfunction in cancer. *Cancer Cell.* **2018**;33:547–562.
 51. Scrimieri F, Askew D, Corn DJ, Eid S, Bobanga ID, Bjelac JA, Tsao ML, Allen F, Othman YS, Wang SC, et al. Murine leukemia virus envelope gp70 is a shared biomarker for the high-sensitivity quantification of murine tumor burden. *Oncoimmunology.* **2013**;2:e26889.
 52. Pilonis KA, Aryankalayil J, Babb JS, Demaria S. Invariant natural killer T cells regulate anti-tumor immunity by controlling the population of dendritic cells in tumor and draining lymph nodes. *J Immunother Cancer.* **2014**;2:37.
 53. Gabrilovich DI. Myeloid-derived suppressor cells. *Cancer Immunol Res.* **2017**;5:3–8.
 54. Youn JI, Nagaraj S, Collazo M, Gabrilovich DI. Subsets of myeloid-derived suppressor cells in tumor-bearing mice. *J Immunol.* **2008**;181:5791–5802.
 55. Allard B, Allard D, Buisseret L, Stagg J. The adenosine pathway in immuno-oncology. *Nat Rev Clin Oncol.* **2020**;17:611–629.
 56. Wennerberg E, Spada S, Rudqvist NP, Lhuillier C, Gruber S, Chen Q, Zhang F, Zhou XK, Gross SS, Formenti SC, et al. CD73 blockade promotes dendritic cell infiltration of irradiated tumors and tumor rejection. *Cancer Immunol Res.* **2020**;8:465–478.
 57. Martinek J, Wu TC, Cadena D, Banchereau J, Palucka K. Interplay between dendritic cells and cancer cells. *Int Rev Cell Mol Biol.* **2019**;348:179–215.
 58. Lee YS, Radford KJ. The role of dendritic cells in cancer. *Int Rev Cell Mol Biol.* **2019**;348:123–178.
 59. Kennedy BE, Sadek M, Elnenaei MO, Reiman A, Gujar SA. Targeting NAD(+) synthesis to potentiate CD38-based immunotherapy of multiple myeloma. *Trends Cancer.* **2020**;6:9–12.
 60. Ribas A, Wolchok JD. Cancer immunotherapy using checkpoint blockade. *Science.* **2018**;359:1350–1355.
 61. Boutros C, Tarhini A, Routier E, Lambotte O, Ladurie FL, Carbonnel F, Izzeddine H, Marabelle A, Champiat S, Berdelou A, et al. Safety profiles of anti-CTLA-4 and anti-PD-1 antibodies alone and in combination. *Nat Rev Clin Oncol.* **2016**;13:473–486.
 62. Hellmann MD, Ciuleanu TE, Pluzanski A, Lee JS, Otterson GA, Audigier-Valette C, Minenza E, Linardou H, Burgers S, Salman P, et al. Nivolumab plus ipilimumab in lung cancer with a high tumor mutational burden. *N Engl J Med.* **2018**;378:2093–2104.
 63. Wolchok JD, Kluger H, Callahan MK, Postow MA, Rizvi NA, Lesokhin AM, Segal NH, Ariyan CE, Gordon RA, Reed K, et al. Nivolumab plus ipilimumab in advanced melanoma. *N Engl J Med.* **2013**;369:122–133.
 64. Gray JE, Villegas A, Daniel D, Vicente D, Murakami S, Hui R, Kurata T, Chiappori A, Lee KH, Cho BC, et al. Three-year overall survival with durvalumab after chemoradiotherapy in stage III NSCLC-update from PACIFIC. *J Thorac Oncol.* **2020**;15:288–293.
 65. Le Mercier I, Chen W, Lines JL, Day M, Li J, Sergent P, Noelle RJ, Wang L. VISTA regulates the development of protective antitumor immunity. *Cancer Res.* **2014**;74:1933–1944.
 66. Ghiringhelli F, Larmonier N, Schmitt E, Parcellier A, Cathelin D, Garrido C, Chauffert B, Solary E, Bonnotte B, Martin F. CD4+CD25+ regulatory T cells suppress tumor immunity but are sensitive to cyclophosphamide which allows immunotherapy of established tumors to be curative. *Eur J Immunol.* **2004**;34:336–344.
 67. Viaud S, Saccheri F, Mignot G, Yamazaki T, Daillère R, Hannani D, Enot DP, Pflirschke C, Engblom C, Pittet MJ, et al. The intestinal microbiota modulates the anticancer immune effects of cyclophosphamide. *Science.* **2013**;342:971–976.
 68. Vanpouille-Box C, Alard A, Aryankalayil MJ, Sarfraz Y, Diamond JM, Schneider RJ, Inghirami G, Coleman CN, Formenti SC, Demaria S. DNA exonuclease Trex1 regulates radiotherapy-induced tumour immunogenicity. *Nat Commun.* **2017**;8:15618.
 69. Gao J, Ward JF, Pettaway CA, Shi LZ, Subudhi SK, Vence LM, Zhao H, Chen J, Chen H, Efstathiou E, et al. VISTA is an inhibitory immune checkpoint that is increased after ipilimumab therapy in patients with prostate cancer. *Nat Med.* **2017**;23:551–555.
 70. Blando J, Sharma A, Higa MG, Zhao H, Vence L, Yadav SS, Kim J, Sepulveda AM, Sharp M, Maitra A, et al. Comparison of immune infiltrates in melanoma and pancreatic cancer highlights VISTA as a potential target in pancreatic cancer. *Proc Natl Acad Sci U S A.* **2019**;116:1692–1697.
 71. Nickols NG, Ganapathy E, Nguyen C, Kane N, Lin L, Diaz-Perez S, Nazarian R, Mathis C, Felix C, Basehart V, et al. The intraprostatic immune environment after stereotactic body radiotherapy is dominated by myeloid cells. *Prostate Cancer Prostatic Dis.* **2020.**
 72. Vatner RE, Formenti SC. Myeloid-derived cells in tumors: effects of radiation. *Semin Radiat Oncol.* **2015**;25:18–27.
 73. Ahn GO, Tseng D, Liao CH, Dorie MJ, Czechowicz A, Brown JM. Inhibition of Mac-1 (CD11b/CD18) enhances tumor response to radiation by reducing myeloid cell recruitment. *Proc Natl Acad Sci U S A.* **2010**;107:8363–8368.
 74. Xu J, Escamilla J, Mok S, David J, Priceman S, West B, Bollag G, McBride W, Wu L. CSF1R signaling blockade stanches tumor-infiltrating myeloid cells and improves the efficacy of radiotherapy in prostate cancer. *Cancer Res.* **2013**;73:2782–2794.

75. Liang H, Deng L, Hou Y, Meng X, Huang X, Rao E, Zheng W, Mauceri H, Mack M, Xu M, et al. Host STING-dependent MDSC mobilization drives extrinsic radiation resistance. *Nat Commun.* 2017;8:1736.
76. Loyher PL, Rochefort J, Baudesson de Chanville C, Hamon P, Lescaille G, Bertolus C, Guillot-Delost M, Krummel MF, Lemoine FM, Combadiere C, et al. CCR2 influences T regulatory cell migration to tumors and serves as a biomarker of cyclophosphamide sensitivity. *Cancer Res.* 2016;76:6483–6494.
77. Mondini M, Loyher PL, Hamon P, Gerbe de Thore M, Laviro M, Berthelot K, Clemenson C, BL S, Combadiere C, Deutsch E, et al. CCR2-dependent recruitment of tregs and monocytes following radiotherapy is associated with tnfa-mediated resistance. *Cancer Immunol Res.* 2019;7:376–387.